26-028

Effect of Soil Amendments on Short-Term CO2 Fluxes in Revegetation Mine Soil

Wilson W. Zoogah
Department of Mining and Explosives Engineering, Missouri University of Science and Technology, Rolla, MO

Abdullah Al Moinee
Department of Mining and Explosives Engineering, Missouri University of Science and Technology, Rolla, MO

Kwame Awuah-Offei
Department of Mining and Explosives Engineering, Missouri University of Science and Technology, Rolla, MO

Mariam K. Al-Lami
Department of Civil, Architectural and Environmental Engineering, Missouri University of Science and Technology, Rolla, MO

Joel G. Burken
Department of Civil, Architectural and Environmental Engineering, Missouri University of Science and Technology, Rolla, MO

ABSTRACT

Soil CO_2 flux serves a critical indicator of ecosystem function and carbon cycling in disturbed landscapes. This study measured and quantified temporal patterns and environmental drivers of soil respiration across fifteen revegetated treatment plots over a 12-week period (July-October 2025). Utilizing automated CO_2 flux measurements, we investigated differences between treatments and quantified their relationships with soil temperature, moisture, and atmospheric pressure. One-way ANOVA revealed significant treatment effects on CO_2 flux ($F_{4,\ 442}$ =14.1, p < 0.001, η^2=0.113), with amended plots exhibiting 40–50% higher mean fluxes than control plots. Weekly temporal analysis demonstrated distinct temporal patterns, with peak fluxes registering in mid-August before a gradual decline. Multiple regression analyses showed that soil temperature (β=0.043, p < 0.001) and moisture (β=2.31, p < 0.001) are the primary flux drivers, together accounting for 18.2% of total variability (adjusted R^2=0.182). Atmospheric pressure had a moderate effect (β=1.13, p < 0.001), detectable only in multivariable analysis. Variance partitioning indicated that environmental factors explained more variability (18.7%) than treatment effect (10.5%), with approximately 71% of flux variability attributed to finer spatial or temporal variability. These results demonstrate that revegetation amendments enhance soil biological activity and impact geochemical cycling, and that temperature and moisture are dominant controls on respiration dynamics in reclaimed mine soils. The findings provide quantifiable benchmarks for ecosystem recovery through altering soil biology and geochemistry and for quantifying carbon sequestration potential in post-mining landscapes.

Keywords: soil respiration, mine reclamation, biochar, arbuscular mycorrhizal fungi, carbon cycling, ANOVA

INTRODUCTIONº

Mining operations generally alter soil structure, biogeochemistry, and ecosystem functioning, creating landscapes with impaired nutrient cycling and reduced carbon storage (Shrestha and Lal 2011; Ussiri and Lal 2005; Pamucar et al. 2025). Surface mining removes topsoil and vegetation, compacts the subsoil, and alters substrate properties, hindering vegetation establishment and microbial activity (Akala and Lal 2001; Zipper et al. 2011). Revegetation is the primary approach for ecosystem restoration; however, the processes and environmental drivers of soil respiration recovery remain poorly understood across different amendment treatments. Substantial needs remain for better understanding amendment approach for increasing soil health and sustained ecological benefit.

Soil CO_2 flux provides an integrated measure of autotrophic (root) and heterotrophic (microbial) components of respiration, providing insight into plant productivity and decomposition processes (Raich and Schlesinger 1992; Hanson et al. 2000). In natural ecosystems, soil respiration typically presents 50–80% of ecosystem respiration and constitutes the second-largest carbon flux in terrestrial systems after gross primary productivity (Bond–Lamberty and Thomson 2010). Understanding the effects of revegetation treatments on soil respiration is essential for predicting long–term carbon sequestration potential and guiding effective restoration strategies in post–mining landscapes (Shang et al. 2024; Bo et al. 2024).

In natural ecosystems, soil respiration is strongly controlled by environmental factors such as temperature and moisture and typically shows a highly nonlinear response to changes in these drivers (Lloyd and Taylor 1994; Davidson et al. 1998; Moyano et al. 2013). Temperature influences enzymatic reaction rates governing decomposition, typically producing a 1.5–3.0-fold increase in respiration per 10°C temperature rise (Q_{10} effect) (Davidson et al. 2006). Other factors include atmospheric pressure, nutrient availability, and biological processes (Jarvis et al. 2007; Manzoni et al. 2012). In disturbed mine soils, however, compaction, altered hydrology, nutrient imbalances, and microbial community disruption can weaken these relationships (Akala and Lal 2001; Mathiba and Awuah–Offei 2015; Hou et al. 2024). Mine soils, in particular, exhibit high bulk density, poor aeration and drainage, restricted rooting depth, low organic matter content, and severe nutrient deficiency (notably nitrogen and phosphorus). Together, these conditions alter the way environmental drivers regulate soil respiration (Sheoran et al. 2010).

Despite the extensive literature on soil respiration in natural ecosystems and some research on reclaimed mine soils, the relative influence of revegetation treatments versus environmental controls on CO_2 flux patterns in revegetated mine soils remains poorly understood. While previous studies have documented elevated respiration (Ros et al. 2003; Li et al. 2024; Mathiba and Awuah–Offei 2015), few have rigorously compared multiple amendment strategies within a single revegetated mine setting or quantified the relative contribution of treatment versus environmental effects on flux variability. Therefore, this study measured soil respiration across fifteen plots representing five different treatment combinations to determine temporal patterns and compare how treatments and environmental drivers influence soil respiration.

The study had three main objectives:

1. Quantify temporal patterns in soil CO_2 flux among different revegetation treatments during the growing season.
2. Evaluate the relative influence of soil temperature, moisture, and atmospheric pressure on flux magnitude
3. Partition variance to assess the relative importance of treatment effects versus environmental controls.

We hypothesized that:

- H1: Amended plots would exhibit higher CO_2 flux due to elevated microbial activity and root biomass.
- H2: Soil temperature and moisture would explain most of the temporal variation, with approximately equal importance.
- H3: Environmental factors would account for more variation in flux than treatment effects, reflecting the dominant role of short-term environmental variability in controlling soil respiration.

MATERIALS AND METHODS

Site Description

We conducted this study at the Sweetwater Mine Site located in Reynolds County, Missouri, USA (approximately 37°21′32″ N, 91°8′48″ W). The site is part of Viburnum Trend lead–zinc mineral belt in southeastern Missouri. The study area lies within the Ozark Highlands Ecoregion, where soils are derived from cherty carbonate parent materials; chert fragments commonly comprise ~20–60% of the soil mass (Chapman et al., 2002; Krusekopf, 1962). Table 1 summarizes the baseline soil characteristics prior to the plot establishment. The collected soil exhibited an acidic pH (4.6) and neutralizable acidity (NA) of 6.1 meq/100g and heavy metal concentrations were within regional background levels.

Experimental Setup and Amendment Applications

We based amendment selection and application rates on previous greenhouse studies of mine tailings (Al–Lami, et al, 2019, 2021, 2022a, 2022b; Kettler, et al, 2025). In Spring 2023, we established plots to evaluate the effects of lime (L), manure (M), woodchips (W), biochar (B), and arbuscular mycorrhizal fungi (AMF) on native prairie establishment in reclaimed mine soils. The area received two herbicide applications in 2022, followed by soil discing and amendment incorporation (to 6 in depth) between February 28

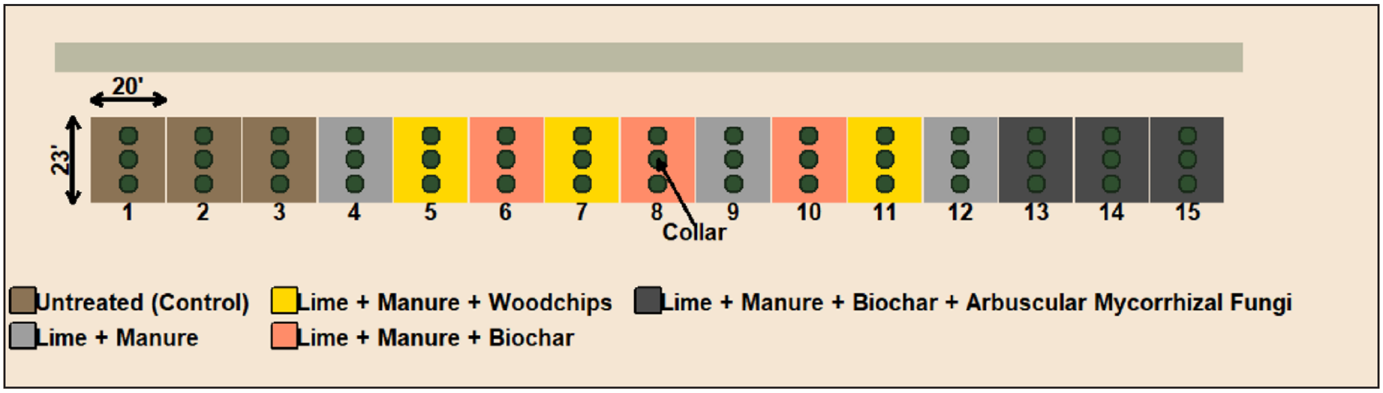

Figure 1. Diagram of experimental design

and March 1, 2023. We established 15 experimental plots (20 ft × 23 ft each, with 4-ft spacing) in a completely randomized design (CRD) consisting of five treatment groups and three replicates per treatment (Figure 1). We applied amendments at equivalent rates in ton/acre for lime (~1), cow manure (~23), hardwood woodchips (~12), and pine–based biochar (~12). On April 25, 2023, we incorporated AMF inoculum at 0.22 ton/acre equivalent rate to approximately 1.5 in depth and seeded all plots with native prairie plant species using a seed drill at the rates listed in the Appendix Table A1.

CO_2 Flux Measurements and Quality Control

We measured soil CO_2 flux using an automated LI–8100A chamber-based system (LI-COR Biosciences, Lincoln, NE, USA) with infrared gas analyzer detection. The response variable, FCO_2 DRY, represents the dry molar flux of CO_2 from the soil surface (μmol·m^{-2}s^{-1}), corrected for atmospheric pressure and temperature with 2–minute chamber closure per reading.

We installed PVC collars with a diameter of 20 cm to 2–8 cm depth in the plot centers, positioned 5 ft from the edge and 6.5 ft apart. We allowed the collars to equilibrate 24 hours before the first measurement. The setup included 45 sampling points (3 per plot) as shown in Figure 1. The system simultaneously recorded soil temperature (°C) and volumetric water content (%VWC) as well as atmospheric pressure (kPa).

We applied rigorous quality filters and retained only readings with $R^2 > 0.98$. We collected data weekly from July 4 to October 3, 2025, for 12 weeks (91 days). The initial dataset contained 540 observations. After filtering, we retained 447 high-quality readings (81–95 per treatment), with CO_2 flux ranging from 0.66 to 7.68 μmol·m^{-2} s^{-1}.

Table 1. Characterization of soil samples collected from the Sweetwater Site (10 cm top layer) prior to revegetation plot establishment

Parameter	Sweetwater Soil*	Background Levels‡
pH (H_2O)	4.6 ± 0.3	>6.1§
NA meq/100g†	6.1 ± 1.7	—
CEC (cmol$^+$ kg^{-1})	10.4 ± 0.9	5–25**
OM (%)[d]	1.3 ± 0.3	—
Ca (mg kg^{-1})	442.5 ± 84.3	—
Mg (mg kg^{-1})	226.9 ± 38.6	—
K (mg kg^{-1})	87.4 ± 23.2	—
NH_4^+–N (mg kg^{-1})	2.8 ± 0.8	—
NO_3^-–N (mg kg^{-1})	7.5 ± 4.0	—
P–Bray (mg kg^{-1})	22 ± 13.1	—
Elements (mg kg^{-1})		
Pb	36.5 ± 9.7	20
Cu	10.6 ± 2.6	13
Cd	0.36 ± 0.12	<1
Zn (extractable)	3.3 ± 4.9	—

*Values represent (mean ± sd), n=5
†NA= Neutralizable Acidity
‡Background concentration for metals in Missouri soils (Tidball 1984)
§Summary of soil fertility status in Missouri (Nathan et al. 2007)
**Scrivner and Cooper 1985

Environmental Variables

We recorded environmental data with integrated sensors: T1 soil temperature at 5 cm depth (°C), V4 (sensor voltage, an indirect moisture proxy), and atmospheric pressure converted to kilopascals (kPa). We pre-calibrated the sensors before deployment and performed the data screening for outliers using a 3–standard deviation threshold.

Statistical Analysis

We used a one-way ANOVA model to test the effects on CO_2 flux with the following factors:

$$Y_{ij} = \mu + \tau_i + \mu_{ij} \quad (1)$$

where Y_{ij} is observation of CO_2 flux for a jth replicate in ith treatment group. The μ is overall mean flux. The τ_i is the effect of ith treatment, for $i = 1\ldots, 5$. The ε is a random error. Constraints

$$\sum n_i \tau_i = 0 \quad (2)$$

ensure model identifiability. Model assumptions require that errors are randomly and independently distributed as follows:

$$\varepsilon_{ij} \sim N(0, \sigma^2) \quad (3)$$

We verified model assumptions and normality of errors prior to ANOVA with (1) the Shapiro–Wilk test for normality at the level of significance of 0.05, (2) Levene's test for homogeneity of variance at the level of significance of 0.05; and (3) visual inspection of residual plots (Fox and Weisberg 2019). We calculated the effect sizes (η^2) and performed Tukey's HSD post–hoc test at $\alpha = 0.05$ to determine which individual treatment groups were significantly different from each other while controlling the family–wise error rate.

While the temporal structure is non–trivially related to the independence assumption, the 12 weekly soil CO_2 flux measurements from the same plots tend to create potential temporal autocorrelation. Specifically, the research team was unable to conduct measurements for some weeks due to the malfunction of the data communication cable between the instrument and laptop and need for replacement during two measurement periods and severe weather conditions during one period, which created missing data for those three time points.

The sufficiently balanced design averages 81–95 samples per treatment and a large total sample size n = 447 confers robustness to moderate temporal autocorrelation (Lumley et al. 2002), and preliminary analysis indicates the consistent rank order of the treatments over time and treatment effects are thus stable rather than dynamic. While the temporal autocorrelation can increase unexplained variance, the highly significant treatment effects $p < 0.001$ remain robust to this conservative concern.

To assess environmental controls on CO_2 flux, we employed a hierarchical approach. First, bivariate relationships were quantified using both Pearson correlation (r, parametric) and Spearman rank correlation (ρ, nonparametric) to assess linear and monotonic relationships, respectively. Second, simple linear regressions were fitted for each environmental predictor individually. Third, a multiple linear regression model incorporating all three environmental variables simultaneously was constructed.

$$\mathbf{FCO_2\ DRY} = \beta_0 + \beta_1(T1) + \beta_2(V4) + \beta_3(\text{Pressure kPa}) + \varepsilon \quad (4)$$

We tested model diagnostics using residual analysis, Cook's distance, and variance inflation factors (VIF < 5). We computed robust standard errors Heteroscedasticity–consistent (HC3 estimator) (Zeileis 2004), standardized and calculated regression coefficients using z–score and validated model generalizability with 10–fold cross-validation.

Finally, we compared adjusted R^2 values from ANOVA model, the multiple regression model and the ANCOVA model. We calculated weekly mean CO_2 flux and visualized results with standard error bands in R version 4.5.1.

RESULTS

Descriptive Statistics

Carbon dioxide (CO_2) flux ranged from 0.66 to 7.68 $\mu mol \cdot m^{-2} \cdot s^{-1}$, (mean of 3.39 ± 1.32 (SD) $\mu mol \cdot m^{-2} \cdot s^{-1}$ (n=447). The distribution showed slight positive skewness (0.53), and mild negative kurtosis (kurtosis = –0.15). The coefficient of variation (38.8%) reflects considerable variability from treatment effects and temporal dynamics (Appendix, Tables A2 & A3).

Assumption Testing

The Shapiro–Wilk test indicated departure from normality (W = 0.966, $p < 0.001$). Given large sample size (n=447) and the robustness of ANOVA to moderate non–normality (Lumley et al. 2002), we proceeded with parametric testing. Levene's test confirmed homogeneity of variance ($F_{4, 442} = 1.37$, $p = 0.243$). The variance ratio among treatments (max/min = 1.38) was well below 3.0. Visual inspection revealed no severe violations (Appendix, Table A4 & A5)

Treatment Effects on CO_2 Flux

One–way ANOVA revealed significant differences among five treatment groups and CO_2 flux ($F_{4,442} = 14.1$, $p < 0.001$). Effect size ($\eta^2 = 0.113$) indicates that treatment explained 11.3% of total variance. Table 2 presents descriptive statistics. The compact letter display refers to the treatment groups which differ, due to the same letter not differing at $\alpha = 0.05$. We present descriptive statistics by

Table 2. Descriptive statistics and Tukey HSD grouping for CO_2 flux by treatment

Treatment	n	Mean ($\mu mol\ m^{-2}s^{-1}$)	SD	SE	Tukey Group
L+M+W	89	4.07	1.35	0.14	c
L+M+B	92	3.52	1.21	0.13	b
L+M+B+AMF	95	3.46	1.22	0.13	b
L+M	81	3.16	1.15	0.13	ab
Untreated	90	2.73	1.27	0.13	a

*Treatments sharing the same letter are not statistically significant.

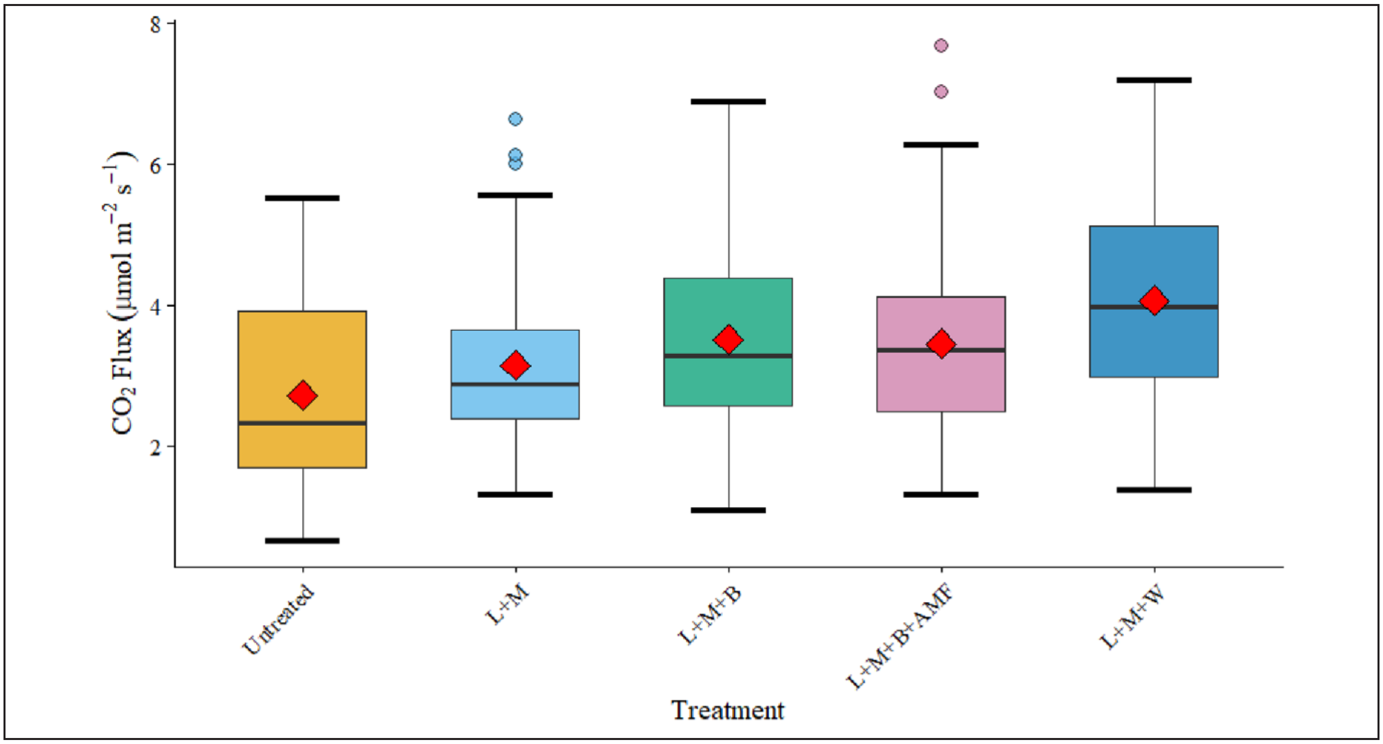

Figure 2. Box–plot comparison of CO_2 flux across five treatment groups

treatment and ANOVA test results in Appendix, Tables A3 & A6, respectively.

The L+M+W (Lime + Manure + Woodchips) treatment exhibited the highest mean flux (4.07 ± 0.14 $\mu mol \cdot m^{-2} \cdot s^{-1}$) and differed significantly from all other treatments. Biochar treatments L+M+B (3.52 ± 0.13 $\mu mol \cdot m^{-2}s^{-1}$) and L+M+B+AMF (3.46 ± 0.13 $\mu mol \cdot m^{-2}s^{-1}$) had a moderate effect compared to the L+M treatment but significantly higher than the control treatment. The manure and lime treatment L+M (3.16 ± 0.13 $\mu mol \cdot m^{-2}s^{-1}$) showed intermediate flux not statistically significant from the untreated control. Additionally, the untreated plots 2.73 ± 0.13 $\mu mol \cdot m^{-2}s^{-1}$) resulted in significantly lower CO_2 flux compared to all amended treatments except the manure and lime treatment L+M.

Pairwise Comparisons

The treatment combined lime, manure, and woodchips (i.e., L+M+W) exceeded the untreated control by 1.35 $\mu mol \cdot m^{-2} \cdot s^{-1}$, 95% CI: 0.84–1.86, $p < 0.001$, representing a 49% increase in CO_2 flux. Biochar–based amended plots L+M+B exceeded the untreated control by 0.79 and L+M+B+AMF by 0.73 $\mu mol \cdot m^{-2} \cdot s^{-1}$, $p < 0.001$. The treatment L+M+W exceeded L+M by 0.91 $\mu mol \cdot m^{-2} \cdot s^{-1}$, $p < 0.001$, L+M+B by 0.55, $p = 0.024$; and exceeded L+M+B+AMF by 0.61, $p = 0.008$. The two biochar treatments showed no difference (–0.06) $\mu mol \cdot m^{-2} \cdot s^{-1}$, $p > 0.998$. Figure 2 presents the box–plot comparison of CO_2 flux across the five treatment groups, and Appendix Table A7 provides the complete pairwise comparison.

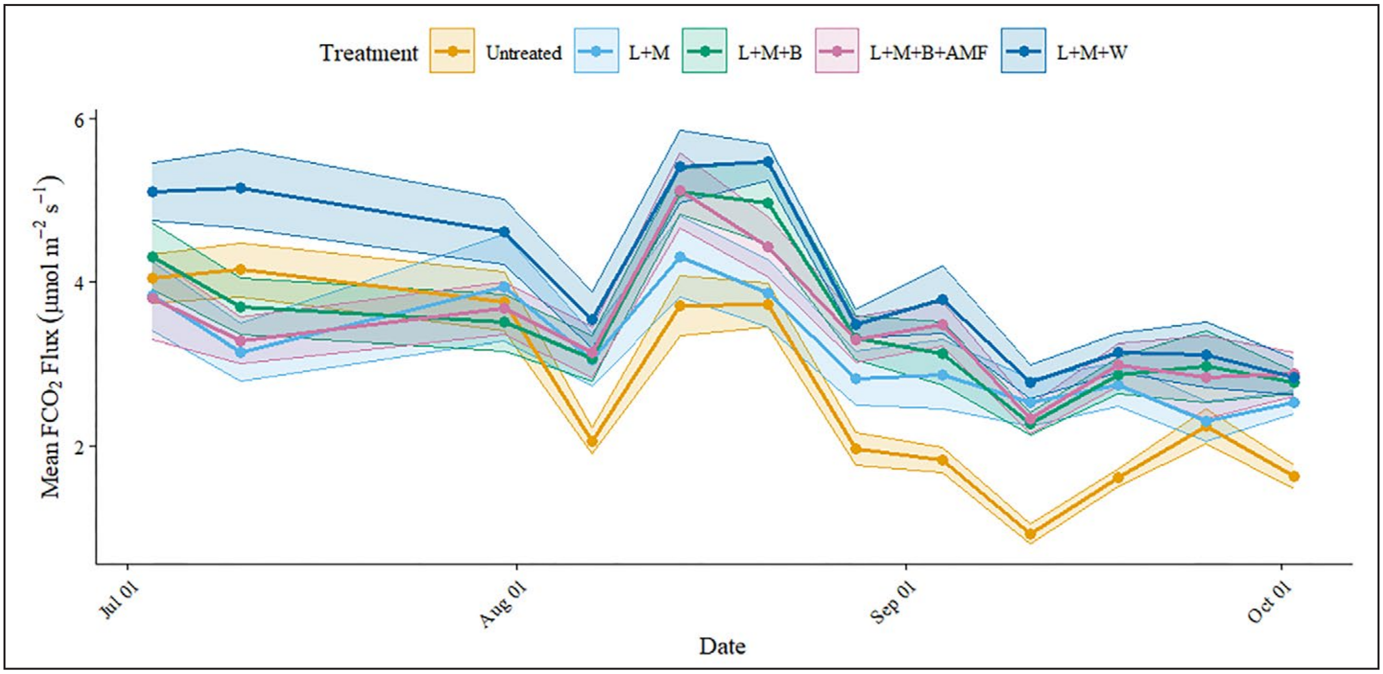

Figure 3. Weekly mean soil CO_2 flux ± SE for the five treatment groups over the 12 weeks period. The lines indicate the temporal patterns, with peaks occurring in mid–August and subsequent declines. The treatment rank order was consistent throughout the observational period

Temporal Dynamics

Weekly mean CO_2 flux showed distinct temporal patterns (Figure 3). We observed stable fluxes in early July ranging from 2–3.5 μmol·m^{-2}·s^{-1}, followed by a rapid increase in mid–August reaching 5–6 μmol·m^{-2}·s^{-1} in the amended plots. This coincided with maximum soil temperatures and optimal moisture conditions. Subsequently, after the August peak, the flux declined progressively in September to early October, averaging 2–3 μmol·m^{-2}·s^{-1}, a 40–50% reduction. This decrease may be due to decreased root activity as plants began to senescence and a reduction in microbial metabolism as temperatures decreased.

The temporal pattern was remarkably consistent across treatments; all plots followed a similar phenological trajectory. However, amended plots consistently maintained higher absolute flux values; The treatment rank order from highest to lowest flux was L+M+W > L+M+B ≈ L+M+B+AMF > L+M > Untreated. This similarity between amended plots and untreated suggests that amendment effects are maintained regardless of the environmental conditions. The untreated reached the lowest flux at all time points and experienced a steeper proportional decline towards the end of the season; 60% from peak to minimum compared to 40–50% in the amended plots. This decline indicates low ecosystem robustness or productivity relative to other treatments.

Environmental Controls on CO_2 Flux

Correlation Analysis

Soil temperature (T1) and sensor voltage (V4, which is a proxy for moisture), showed moderate positive correlations with CO_2 flux. Pearson's correlations were r = 0.326 for T1 and r = 0.275 for V4 ($p < 0.0001$), indicating that these factors explained approximately 10.6% and 7.6% of the variance in flux respectively. Spearman's correlations confirmed relatively linear monotonic relationships (ρ = 0.310 and 0.290, respectively). All illustrations are in Table 3.

Atmospheric pressure had a weak, non–significant bivariate correlation (Pearson r = 0.083, p = 0.080; Spearman's ρ = 0.076, p = 0.111). However, multiple regression results suggested a statistical suppression in which the pressure effect was only detectable after controlling temperature and moisture.

Simple Linear Regressions

Simple linear regression models identified distinct environmental influences on CO_2 flux (Table 4). Soil temperature was responsible for 10.6% of flux variance (R^2 = 0.106, adjusted R^2 = 0.104). Each 1°C increase in temperature corresponded to a 0.045 μmol·m^{-2}·s^{-1} increase in flux (β = 0.045, SE = 0.0062, t = 7.26, $p < 0.0001$). A Q_{10} of approximately 1.6–2.0 indicates that this effect is typical for soil respiration throughout the growing season.

Sensor voltage (V4) accounted for 7.6% of flux variance (R^2 = 0.076, adjusted R^2 = 0.074). Each 1–volt increase in V4 corresponded to a 2.50 μmol·m^{-2}·s^{-1} increase in flux (β = 2.505, SE = 0.4149, t = 6.04, $p < 0.0001$). This positive relationship indicates that CO_2 flux increased as soils became drier because higher v4 values represent drier soil conditions— likely reflect enhanced aerobic respiration under greater oxygen availability in drier soils which supports higher microbial activity and CO_2 production. In contrast atmospheric pressure revealed only 0.7% of variance (R^2 = 0.007), and showed no significant effect (β = 0.500, SE = 0.2853, t = 1.75, p = 0.080).

The multiple regression model in Figure 4 explained substantially more variance than any single predictor R^2 = 0.187, adjusted R^2 = 0.182, $F_{3,\ 443}$ = 33.98, $p < 0.0001$, RMSE = 1.19 μmol·$m^{-2}s^{-1}$. This improvement in model

Table 3. Pearson and Spearman correlation between CO_2 flux and environmental variables

Variable	Method	r or ρ	p–value	n
Soil Temperature (T1, °C)	Pearson	0.326	< 0.0001	447
Soil Temperature (T1, °C)	Spearman	0.310	< 0.0001	447
Soil Moisture (V4, V)	Pearson	0.275	< 0.0001	447
Soil Moisture (V4, V)	Spearman	0.290	< 0.0001	447
Atmospheric Pressure (kPa)	Pearson	0.083	0.080	447
Atmospheric Pressure (kPa)	Spearman	0.076	0.111	447

Note: Soil moisture sensor voltage (V4) is inversely proportional to soil water content: higher voltage indicates drier conditions

Table 4. Simple linear regression results for environmental predictors of CO_2 flux

Predictor	Intercept	Slope (β)	SE(β)	t	p–value	R^2	Adj. R^2	RMSE
Temperature (T1)	1.592	0.045	0.0062	7.26	<0.0001	0.106	0.104	1.25
Moisture (V4)	1.462	2.505	0.4149	6.04	<0.0001	0.076	0.074	1.27
Pressure	–44.388	0.500	0.2853	1.75	0.080	0.007	0.005	1.31

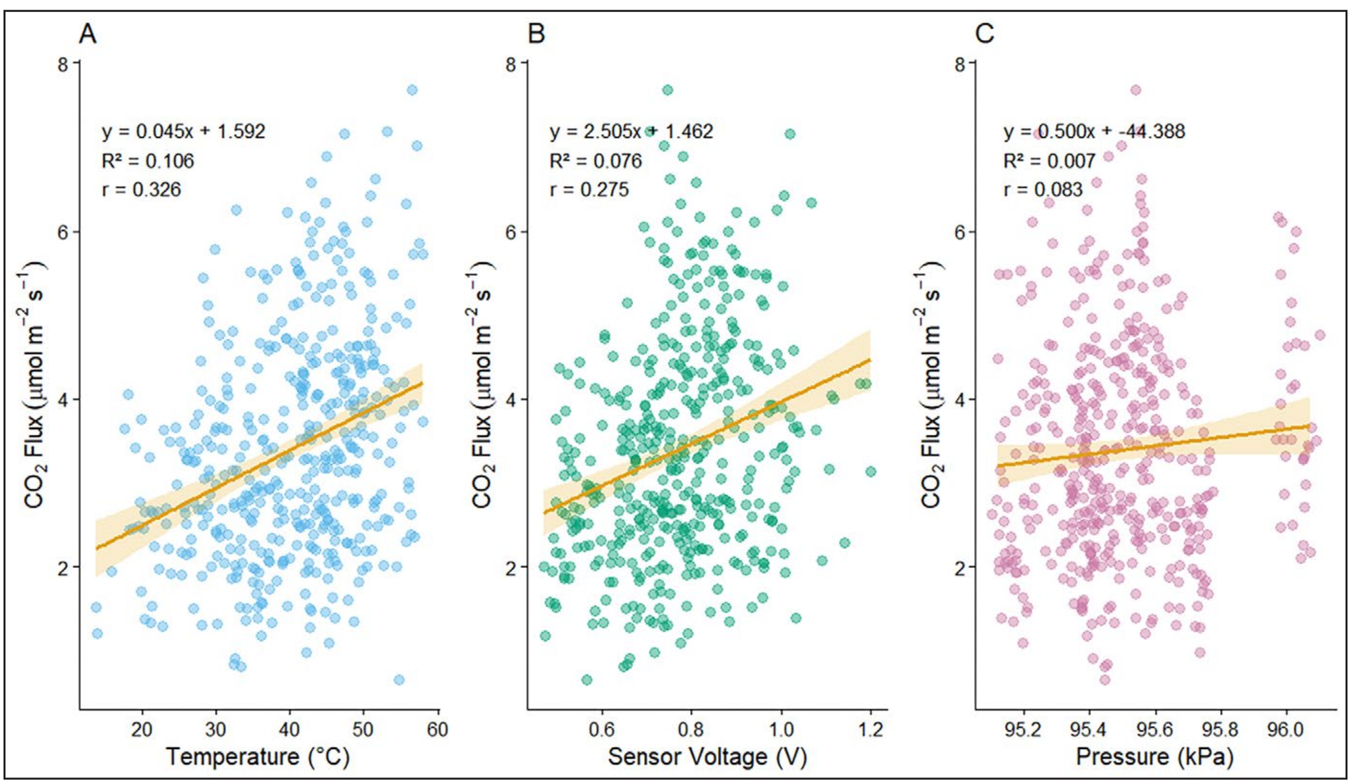

Figure 4. The relationships between soil CO_2 flux and simple linear regression fits (Temperature (A), Sensor Voltage (B) and Pressure (C))

Table 5. Multiple regression model: CO_2 flux as function of environmental variables

Term	Estimate	SE	t–value	p–value	Standardized β	VIF
Intercept	–107.616	25.5300	–4.22	< 0.0001	—	—
Soil Temperature (T1)	0.043	0.0061	7.10	< 0.0001	0.312	1.06
Soil Moisture (V4)	2.314	0.4020	5.76	< 0.0001	0.254	1.06
Atmospheric Pressure	1.126	0.2660	4.23	< 0.0001	0.186	1.06

Model Statistics: $R^2 = 0.187$, Adjusted $R^2 = 0.182$, $F_{3,443} = 33.98$, $p < 0.0001$, RMSE = 1.19 $\mu mol \cdot m^{-2} \cdot s^{-1}$(Appendix A9).

performance indicates that temperature, moisture, and atmospheric pressure jointly provide a more comprehensive explanation of CO_2 flux variation than any single factor alone.

When we considered all three variables simultaneously, they still significantly explained CO_2 flux. The coefficient for soil temperature was $\beta = 0.043$ $\mu mol \cdot m^{-2} \cdot s^{-1} \cdot °C^{-1}$ (SE = 0.0061, t = 7.10, $p < 0.0001$), indicating that flux increases by 0.043 $\mu mol \cdot m^{-2} \cdot s^{-1}$ for each 1°C rise in temperature. Soil moisture (V4) showed a coefficient of $\beta = 2.314$ $\mu mol \cdot m^{-2} \cdot s^{-1} \cdot V^{-1}$ (SE = 0.402, t = 5.76, $p < 0.0001$), while atmospheric pressure had a coefficient of $\beta = 1.126$ $\mu mol \cdot m^{-2} \cdot s^{-1} \cdot kPa^{-1}$ (SE = 0.266, t = 4.23, $p < 0.0001$). Although atmospheric pressure exhibited no significant bivariate correlation with CO_2 flux, it became significant in the multiple regression model, indicating a suppression effect—that is, pressure influenced flux only after accounting for temperature and moisture.

Figure 4 illustrates the relationships between CO_2 flux and the environmental predictors, with simple linear regression fits and 95% confidence intervals. Standardized regression coefficients in Table 5 enable direct comparison of relative effect sizes. When standardized, soil temperature and soil moisture exerted the strongest influences (Std. β = 0.312), followed by soil moisture (Std. β = 0.254), whereas atmospheric pressure had a weaker effect, corresponding to approximately 60% of the magnitude of temperature and 73% of moisture. The VIF (~1.06) confirmed that multicollinearity was minimal, meaning the three predictors contributed independent information. We summarized the sampling details in Appendix Table A8.

Variance Partitioning

Treatments effects only explained 11.3% of CO_2 flux variance (adjusted R^2 =10.5). Environmental variables alone accounted for 18.2% (adjusted R^2=0.182). The ANCOVA model, which included both treatments and environmental variables, explained 28.9% of the variance (adjusted R^2=0.289), suggesting that their effects were approximately additive. The 1.7:1 ratio between environmental and treatment contributions indicates that short–term environmental fluctuations exert a stronger influence on CO_2 flux than long–term treatment effects. Approximately 71% of flux variability remains unexplained, reflecting spatial heterogeneity, unmeasured variability, temporal dynamics at sub–weekly scales, and natural stochasticity. Appendix Table A10 provides detailed results.

DISCUSSION

Treatment Effects on Soil Respiration

Organic amendments significantly increased soil respiration compared to the control, showing a 40–50% increase in CO_2 flux ($F_{4,442} = 14.1$, $p < 0.001$), indicating a successful stimulation of microbial activities. This is likely due to the enhanced soil physicochemical and biological properties, increased substrate availability, stimulated microbial community and extracellular enzyme activity, greater root biomass and exudation, and induced positive priming of native organic matter in the amended plots (Ros et al. 2003; Sheoran et al. 2010; Li et al. 2024; Pandian et al. 2024; Shang et al. 2024; Zhang, et al 2024).

Among treatments, the combined treatment of lime, manure, and woodchips (i.e., L+M+W) resulted in the highest CO_2 flux and significantly differed from all treatments. Biochar–based treatments (i.e., L+M+B and L+M+B+AMF) were also elevated relative to the control but were intermediate compared to other treatments.

The lime and manure treatment (i.e., L+M), did not differ significantly from the controls, likely due to depletion of labile carbon pools for 2.5 years post application.

Raw carbon–based material such as woodchips may provide easily decomposable organic matter including labile fractions of soluble sugars, hemicelluloses, and cellulose, which microbes can rapidly mineralize (Li et al 2013). Whereas biochar is a highly recalcitrant carbon–based material with elevated sorption capacity impacting the availability of nutrients, dissolved organic carbon and extracellular enzymes, and inducing increased C:N and C:P ratios, thus promoting carbon use efficiency and shaping soil microbial activity (Joseph et al 2021; Jindo et al 2020; Giagnoni, et al 2022; Zeng, et al 2024; Stewart et al. 2007). However, carbon benefits from pyrogenic sources include slower decomposition turnover and an enhanced diversity effect on microbial communities (Thea Whitman et al, 2016).

The absence of difference between biochar treatments with and without AMF (0.06 μmol·m^{-2}·s^{-1}, p=0.998) was surprising, given the reported role of AMF in plant–soil carbon transfer. This result may reflect insufficient time for AMF colonization to affect CO_2 Flux within the 2–3 years (Högberg et al. 2001; Conti et al. 2025; Tang et al. 2025; Du et al. 2025; Li et al. 2025; Zhang et al. 2025). It may also reflect that native AMF populations account for the difference. AMF effects on carbon allocation do not necessarily result in total respiration. Instead, AMF often diverts recent plant C into mycorrhizal hyphal structures, glomalin–related soil proteins, and plant root tissue. Furthermore, AMF may compete with free–living decomposers for N and P, suppressing saprotrophic enzyme activity and reducing positive priming effects (Joseph et al 2021; Jindo et al 2020; Giagnoni, et al 2022; Zeng, et al 2024). Longer–term observations may reveal divergence as AMF network matures.

Temporal Patterns and Phenological Controls

CO_2 flux exhibited a distinct seasonal pattern—remaining stable in July, peaking in mid–August, and progressively declining through autumn, reflects the combined influence of temperature, moisture and plant phenology. The mid–August peak coincided with maximum temperatures, and optimal moisture producing favorable conditions for root and microbial respiration. The gradual reduction of 40–50% likely reflects cooling temperature and lower enzymatic rates, plant senescence reducing autotrophic respiration and decreased substrate inputs (Curiel Yuste et al. 2004; Savage et al. 2008; Vardag et al. 2025).

Amendments effects remained consistent across time, suggesting that organic additions shift baseline respiration rates without altering the fundamental environmental response relationships—a valuable characteristics for restoration management where predictability is important.

Environmental Drivers

The nearly equal standardized effects of temperature and moisture support our hypotheses. The temperature coefficient corresponded to a Q_{10} of approximately 1.6–2.0, within the typical range but toward the lower end, which might indicate a substrate limitation in mine soils constraining temperature sensitivity (Bond–Lamberty and Thomson 2010; Davidson et al. 2006; He et al. 2024).

The positive relationship between sensor voltage (drier conditions) and that of CO_2 requires careful interpretation. This means enough moisture remains to support activity, but well–aerated conditions facilitate oxygen diffusion (Jarvis et al. 2007; Manzoni et al. 2012). The study period (July–October) may not have captured extreme drought that would reverse this relationship.

Atmospheric pressure emerged as a significant predictor only in multiple regression, demonstrating statical suppression. Pressure likely influenced CO_2 flux indirectly via barometric pumping, pressure–mediated alterations in gas solubility, and pressure differences that cause fluctuations in soil gas density (Takle et al. 2004; Flechard et al. 2005; LI–COR Biosciences 2018; Maier et al. 2010). Although the standardized effect is relatively low, and the range of pressure is restrictive (between 95.2 and 96.0 kPa), its detection underscores the sensitivity of multivariate models in identifying subtle drivers.

Variance Partitioning and Implications

Environmental variables explained more variance in CO_2 flux than treatment effects, aligning with predictions that short-term environmental fluctuations dominate flux dynamics. The 1.7:1 ratio between environmental and treatment contributions is a common occurrence in the available records and reports (Bond–Lamberty and Thomson 2010; Li et al. 2024; Vargas et al. 2011). The large population of unexplained variance likely reflects spatial heterogeneity, temporal variability, unmeasured processes, and intrinsic stochasticity in soil systems (Mathiba and Awuah–Offei 2015; Kuzyakov and Gavrichkova 2010).

Nonetheless, treatment effects are profound and have been surprisingly stable across all conditions and times, which confirms the reliability of amendments and the directionality of their effects. The essentially additive nature of treatment and environmental variables makes the overall patterns predictable. Our model's validation provides insights into real world situations in predicting carbon flux dynamics (James et al., 2013).

The results have direct implications for mine reclamation. The enhanced CO_2 flux indicates the successful stimulation of soil biological activity, which is vital for ecosystem recovery (Ussiri and Lal 2005). However, the net carbon balance is determined by gross primary productivity and ecosystem respiration. Thus, higher soil respiration may reflect transient decomposition of added resources that will eventually stabilize with the formation of recalcitrant carbon or a sustained increase in autotrophic respiration due to increased plant productivity (Hanson et al. 2000: Stewart et al. 2007). Distinguishing these processes requires concurrent and long-term measurement of net primary productivity, aboveground biomass, and soil organic carbon stock.

Given the system's high sensitivity to climate variability, treatment selection for restoration projects should be based on multi-year carbon balance outcomes, not short-term CO_2 flux responses. While organic amendments—particularly woodchips—enhance soil function, this study indicates and inspires plannings to evaluate their long-term effect over many years of carbon balance rather than instantaneous flux.

Study Limitation and Future Research

The study's first limitation is the single growing season of CO_2 flux measurements. We require multiple–year observation in order to evaluate treatment effects across varying climate conditions and development stages. The second limitation is that sensor voltage provided only a relative measure of soil moisture; calibration of sensors would enable quantitative evaluation of moisture thresholds and nonlinear responses. The final limitation arises from uneven sample size after quality control data filtering, although statistical balance remained sufficient for robust inference.

Future research studies should aim to 1) conduct seasonal and annual monitoring across full climatic cycles, 2) include comprehensive soil characterization including carbon pool, (labile, total organic carbon, and microbial biomass carbon and 3) partition autotrophic and heterotrophic respiration components to understand mechanisms during the treatment differences.

CONCLUSIONS

Organic amendments (particularly woodchips combined with lime and manure) enhanced soil respiration in reclaimed mine spoil, with 40–50% higher flux than the untreated controls. Treatment effects remained consistent throughout the study period, despite seasonal and temporal fluctuation, demonstrating the robustness and reliability of this amendment in stimulating biological activity. Amendments also impact vegetation profiles and biomass, not shown here. The distinct seasonal pattern of the soil CO_2 flux showed a peak in mid–summer and decline in autumn is attributed to temperature and phenological effect. Soil temperature and soil moisture drove most of the flux variation, together explaining 18.2% of the observed variability, while atmospheric pressure also had a small but noticeable effect. Combining treatment effects with environmental factors explained substantially variance (28.9%) than treatments alone (10.5%), indicating the influence of spatial heterogeneity and temporal variation in fluxes at smaller, though unspecified scales.

These results highlight the value of multi–year, replicated monitoring programs to accurately quantify carbon dynamics for valid estimation and evaluate treatment impacts. In conclusion, the results of this study indeed support that organic amendments are highly prospective treatments for offering effective strategies to activate soil biodiversity and restore ecosystem function in mine reclamation. Yet, complete carbon accounting requires measuring net ecosystem production (NEP) over multiple years in order to estimate both net primary productivity and the amount of carbon sequestered. Long-term monitoring enables researchers and practitioners to distinguish short–term decomposition-driven responses for CO_2 release from stable increases in productivity, allowing reclamation strategies to maximize ecosystem service delivery and contribute meaningfully to regional carbon balance targets under climate change. Achieving these goals along with complementary work on vegetative response and long-term biogeochemical cycling will have a great impact as we look to restore legacy mining sites and improve sustainable mining practices of the future.

ACKNOWLEDGMENTS

We gratefully acknowledged The Doe Run Company for partially sponsoring this research and for granting the research team access to conduct this experiment. We extend our sincere gratitude to the Minerals Commission– Ghana for their support of the research. We also thank Tambudze Tinozivashe for assistance with fieldwork.

REFERENCES

Akala, V.A., and Lal, R. 2001. Soil organic carbon pools and sequestration rates in reclaimed mine soils in Ohio. Journal of Environmental Quality 30(6): 2098–2104.

Al–Lami, Mariam K., et al. "Amendment–assisted revegetation of mine tailings: improvement of tailings quality and biomass production." International Journal of Phytoremediation 21.5 (2019): 425–434.

Al–Lami, Mariam K., et al. "High throughput screening of native species for tailings eco–restoration using novel computer visualization for plant phenotyping." Science of The Total Environment 780 (2021): 146490.

Al–Lami, Mariam K., et al. "Phytomanagement of Pb/Zn/Cu tailings using biosolids–biochar or–humus combinations: Enhancement of bioenergy crop production, substrate functionality, and ecosystem services." Science of the Total Environment 836 (2022): 155676.

Al–Lami, Mariam. Ecological restoration of lead/zinc/copper mine tailings: Phytomanagement and amendment strategies to enhance substrate functionality and biomass production. Missouri University of Science and Technology, 2022.

Bo, H., Xue, D., Li, Z., Wang, H., Jin, D., and Wang, H. 2024. Soil microbial residual carbon accumulation affected by reclamation period and straw incorporation in reclaimed soil from coal mining area. Agronomy 14(4): Article 742.

Bond–Lamberty, B., and Thomson, A. 2010. Temperature–associated increases in the global soil respiration record. Nature 464(7288): 579–582.

Chapman, S.S., Omernik, J.M., Griffith, G.E., Schroeder, W.A., Nigh, T.A., and Wilton, T.F., 2002. Ecoregions of Iowa and Missouri (color poster with map, descriptive text, summary tables, and photographs): Reston, Virginia, U.S. Geological Survey (map scale 1:1,800,000). Available online at: https://www.epa.gov/eco-research/ecoregion-download-files-state-region-7#pane-23. Date accessed: December 8, 2021.

Conti, M., et al. 2025. The potential of arbuscular mycorrhizal fungi to improve soil organic carbon in agricultural ecosystems: A meta–analytical approach. Functional Ecology 39: 14753.

Curiel Yuste, J., Janssens, I.A., Carrara, A., and Ceulemans, R. 2004. Annual Q_{10} of soil respiration reflects plant phenological patterns as well as temperature sensitivity. Global Change Biology 10(2): 161–169.

Davidson, E.A., Belk, E., and Boone, R.D. 1998. Soil water content and temperature as independent or confounded factors controlling soil respiration in a temperate mixed hardwood forest. Global Change Biology, 4(2), 217–227.

Davidson, E.A., Janssens, I.A., and Luo, Y. 2006. On the variability of respiration in terrestrial ecosystems: moving beyond Q_{10}. Global Change Biology 12(2): 154–164.

Du, L., et al. 2025. Harnessing arbuscular mycorrhizal fungal communities for ecological restoration: A conceptual framework. Soil Biology and Biochemistry 204: Article 109968.

Flechard, C.R., Neftel, A., Jocher, M., Ammann, C., and Fuhrer, J. 2005. Bi–directional soil/atmosphere N_2O exchange over two mown grassland systems with contrasting management practices. Global Change Biology 11(12): 2114–2127.

Fox, J., and Weisberg, S. 2019. An R Companion to Applied Regression, Third Edition. Sage Publications, Thousand Oaks, CA.

Giagnoni, L.; Renella, G. Effects of Biochar on the C Use Efficiency of Soil Microbial Communities: Components and Mechanisms. Environments 2022, 9, 138. DOI: 10.3390/environments9110138.

Hanson, P.J., Edwards, N.T., Garten, C.T., and Andrews, J.A. 2000. Separating root and soil microbial contributions to soil respiration: A review of methods and observations. Biogeochemistry, 48(1), 115–146.

He, P., et al. 2024. Straw addition and low soil moisture decreased temperature sensitivity and activation energy of soil organic matter. Geoderma 442: Article 116802.

Hou, D., Xu, M., Wang, M., Li, X., Li, S., Wang, J., and Cao, M. 2024. Research on ecological restoration and green reclamation technology of goaf in phosphorus mines. Frontiers in Environmental Science 12: Article 1343185.

Högberg, P., Nordgren, A., Buchmann, N., Taylor, A.F., Ekblad, A., Högberg, M.N., Nyberg, G., Ottosson–Löfvenius, M., and Read, D.J. 2001. Large–scale forest girdling shows that current photosynthesis drives soil respiration. Nature 411(6839): 789–792.

James, G., Witten, D., Hastie, T., and Tibshirani, R. 2013. An Introduction to Statistical Learning: with Applications in R. Springer, New York, NY.

Jarvis, P., Rey, A., Petsikos, C., Wingate, L., Rayment, M., Pereira, J., Banza, J., David, J., Miglietta, F., Borghetti, M., Manca, G., and Valentini, R. 2007. Drying and wetting of Mediterranean soil stimulates decomposition and carbon dioxide emission: the “Birch effect”. Tree Physiology 27(7): 929–940.

Jindo, K., Audette, Y., Higashikawa, F.S. et al. Role of biochar in promoting circular economy in the agriculture sector. Part 1: A review of the biochar roles in soil N, P and K cycles. Chem. Biol. Technol. Agric. 7, 15 (2020). DOI: 10.1186/s40538-020-00182-8.

Joseph, Stephen, et al. “How biochar works, and when it doesn’t: A review of mechanisms controlling soil and plant responses to biochar.” Gcb Bioenergy 13.11 (2021): 1731–1764.

Kettler, E.M., et al. 2025. Arbuscular mycorrhizal fungi combined with biosolids, and biochar sustained phytostabilization and enhanced soil properties of mine tailings. Poster presented at Miners Solving for Tomorrow Research Conference, Missouri University of Science and Technology, Rolla, MO, April 2.

Kirk, R.E. 2013. Experimental Design: Procedures for the Behavioral Sciences (4th ed.). Sage Publications, Thousand Oaks, CA.

Krusekopf, H. H., 1962. Major Soil Areas of Missouri, 1962. University of Missouri Agricultural Experiment Station B785: May 1962.

Kuzyakov, Y., and Gavrichkova, O. 2010. Time lag between photosynthesis and carbon dioxide efflux from soil: a review of mechanisms and controls. Global Change Biology, 16(12), 3386–3406.

Lehmann, J., and Joseph, S. (Eds.). 2009. Biochar for Environmental Management: Science and Technology. Earthscan, London, UK.

Li, M.Y., Wang, W.Y., Li, S.S., Xiao, Y.L., Yang, C.L., Xiong, Y.C., Zhu, L., Yin, H.H., Tao, H.Y., Chen, Y., and Ashraf, M. 2025. The functional role of arbuscular mycorrhizal fungi in enhancing soil organic carbon stocks and stability in dryland. Soil Biology and Biochemistry 202: Article 108644.

Li, Z., et al. 2024. Assessment of carbon sequestration potential of mining areas under ecological restoration in China. Science of the Total Environment 920: Article 170584.

LI–COR Biosciences. 2018. LI–8100A Automated Soil CO_2 Flux System & LI–8150 Multiplexer Instruction Manual. LI–COR, Inc., Lincoln, NE.

Lloyd, J., and Taylor, J.A. 1994. On the temperature dependence of soil respiration. Functional Ecology 8(3): 315–323.

Lumley, T., Diehr, P., Emerson, S., and Chen, L. 2002. The importance of normality assumption in large public health data sets. Annual Review of Public Health 23(1): 151–169.

Maier, M., Schack–Kirchner, H., Hildebrand, E.E., and Holst, J. 2010. Pore–space CO_2 dynamics in a deep, well–aerated soil. European Journal of Soil Science 61(6): 877–887.

Manzoni, S., Schimel, J.P., and Porporato, A. 2012. Responses of soil microbial communities to water stress: results from a meta-analysis. Ecology 93(4): 930–938.

Mathiba, M.M., and Awuah–Offei, K. 2015. Spatial autocorrelation of soil CO_2 flux on reclaimed mined land: Implications for sampling. Environmental Monitoring and Assessment 187(11): 699.

Moyano, F.E., Manzoni, S., and Chenu, C. 2013. Responses of soil heterotrophic respiration to moisture availability: An exploration of processes and models. Soil Biology and Biochemistry 59: 72–85.

Nathan MV, Sun Y, Dunn D. 2007. Summary of soil fertility status in Missouri by county, soil region and cropping systems. Progress report. [accessed 2018 Nov 7]. http://aes.missouri.edu/pfcs/research/prop907a.pdf (opens in a new window)

Pamucar, D., et al. 2025. Transforming mining–affected lands through eco–friendly reclamation strategies. Ecological Indicators 172: Article 112785.

Pandian, K., Vijayakumar, S., Mustaffa, M.R.A.F., Subramanian, P., and Chitraputhirapillai, S. 2024. Biochar—a sustainable soil conditioner for improving soil health, crop production and environment under changing climate: A review. Frontiers in Soil Science, 4, Article 1376159.

Phillips, C.L., Nickerson, N., Risk, D., Kayler, Z.E., Andersen, C., Mix, A., and Bond, B.J. 2011. Interpreting diel hysteresis between soil respiration and temperature. Global Change Biology 17(1): 515–527.

Raich, J.W., and Schlesinger, W.H. 1992. The global carbon dioxide fluxes in soil respiration and its relationship to vegetation and climate. Tellus B 44(2): 81–99.

Ros, M., Hernandez, M.T., and García, C. 2003. Soil microbial activity after restoration of a semiarid soil by organic amendments. Soil Biology and Biochemistry 35(3): 463–469.

Savage, K., Davidson, E.A., and Tang, J. 2008. Diel patterns of autotrophic and heterotrophic respiration among phenological stages. Global Change Biology 14(7): 1518–1532.

Scrivner CL, Cooper DT. 1985. Organic carbon in soils of Missouri, a summary of accumulated research data. Research Bulletin 1055, Columbia, Missouri, USA. p.7. [accessed 2018 Nov 7]. https://mospace.umsystem.edu/xmlui/bitstream/handle/10355/53309/age001055.pdf?sequence=1&isAllowed=y (opens in a new window)

Shang, Z., et al. 2024. Effects of recultivation on soil organic carbon sequestration in abandoned coal mining sites: A meta-analysis. Scientific Reports 12: Article 22937.

Sheoran, V., Sheoran, A.S., and Poonia, P. 2010. Soil reclamation of abandoned mine land by revegetation: a review. International Journal of Soil, Sediment and Water, 3(2), 13.

Shrestha, R.K., and Lal, R. 2011. Changes in physical and chemical properties of soil after surface mining and reclamation. Geoderma 161(3–4): 168–176.

Stewart, C.E., Paustian, K., Conant, R.T., Plante, A.F., and Six, J. 2007. Soil carbon saturation: concept, evidence and evaluation. Biogeochemistry 86(1): 19–31.

Takle, E.S., Massman, W.J., Brandle, J.R., Schmidt, R.A., Zhou, X., Litvina, I.V., Garcia, R., Doyle, G., and Rice, C.W. 2004. Influence of high–frequency ambient pressure pumping carbon dioxide efflux from

soil. Agricultural and Forest Meteorology 124(3–4): 193–206.
Tang, L., et al. 2025. Mycorrhizal allies: Synergizing Forest carbon and multifunctional restoration. Trends in Ecology & Evolution 40: 188–200.
Thea Whitman, Charles Pepe–Ranney, Akio Enders, Chantal Koechli1, Ashley Campbell, Daniel H Buckley and Johannes Lehmann, 2016. Dynamics of microbial community composition and soil organic carbon mineralization in soil following addition of pyrogenic and fresh organic matter, The ISME Journal (2016) 10: 2918–2930
Tidball RR. 1984. Geochemical survey of Missouri, geography of soil geochemistry of Missouri agricultural soils. Washington, USA: United States government printing office. p. 4–7. https://pubs.usgs.gov/pp/0954h-i/report.pdf (opens in a new window).
Ussiri, D.A.N., and Lal, R. 2005. Carbon sequestration in reclaimed minesoils. Critical Reviews in Plant Sciences, 24(3): 151–165.
Vardag, S.N., et al. 2025. CO_2 release during soil rewetting shapes the seasonal carbon dynamics in South American Temperate region. Geophysical Research Letters, 52, Article e2024GL111725.
Vargas, R., Baldocchi, D.D., Bahn, M., Hanson, P.J., Hosman, K.P., Kulmala, L., Pumpanen, J., and Yang, B. 2011. On the multi–temporal correlation between photosynthesis and soil CO_2 efflux: reconciling lags and observations. New Phytologist 191(4): 1006–1017.
Zeileis, A. 2004. Econometric computing with HC and HAC covariance matrix estimators. Journal of Statistical Software 11(10): 1–17.
Zeng, Lingqun, Andrew R. Zimmerman, and Rixiang Huang. "Adsorption of extracellular enzymes by biochar: Impacts of enzyme and biochar properties." Geoderma 451 (2024): 117082.
Zhang, Y., et al. 2025. Large–scale survey reveals arbuscular mycorrhizal fungi enhance grassland soil carbon storage. Nature Ecology & Evolution 9: 124–132.
Zipper, C.E., Burger, J.A., Skousen, J.G., Angel, P.N., Barton, C.D., Davis, V., and Franklin, J.A. 2011. Restoring forests and associated ecosystem services on Appalachian coal surface mines. Environmental Management 47(5): 751–765.

APPENDICES: STATISTICS (DETAILED TABLES)

Table A1. Revegetation species mix applied at Sweetwater Mine Site

Botanical Name	Common Name	Total Applied (PLS lbs.)
Andropogon gerardii	Big bluestem	2.16
Chasmanthium latifolium	River oats	0.90
Elymus virginicus	Virginia wildrye	0.90
Panicum virgatum	Switchgrass	0.90
Schizachyrium scoparium	Little bluestem	2.16
Sorghastrum nutans	Indian grass	0.90
Asclepias syriaca	Common milkweed	1.80
Asclepias tuberosa	Butterfly milkweed	1.80
Asclepias verticillata	Whorled milkweed	0.90
Chamaecrista fasciculata	Partridge pea	0.90
Coreopsis lanceolata	Lanceleaf coreopsis	0.54
Dalea purpurea	Purple prairie clover	0.90
Desmanthus illinoensis	Illinois bundleflower	0.36
Echinacea pallida	Pale purple coneflower	1.44
Lespedeza capitata	Roundhead lespedeza	1.08
Penstemon digitalis	Foxglove beardtongue	0.18
Rudbeckia hirta	Black–eyed Susan	0.18
Total PLS lbs. Applied		**18.00**

Table A2. Overall descriptive statistics for CO_2 flux (n=447)

Statistic	Value
Sample size (n)	447
Mean	3.39
Median	3.26
Standard Deviation (SD)	1.32
Standard Error (SE)	0.062
Minimum	0.66
Maximum	7.68
First Quartile (Q1)	2.42
Third Quartile (Q3)	4.29
Interquartile Range (IQR)	1.87
Coefficient of Variation (CV, %)	38.8
Skewness	0.53
Kurtosis	–0.15

Table A3. Descriptive statistics by treatment (n=447)

Treatment	n	Mean	SE	Median	SD	Min	Max	Q1	Q3	Group
Untreated	90	2.73	0.13	2.34	1.27	0.66	5.51	1.71	3.52	a
L+M	81	3.16	0.13	2.88	1.15	1.31	6.62	2.39	3.91	ab
L+M+B	92	3.52	0.13	3.28	1.21	1.09	6.88	2.57	4.38	b
L+M+B+AMF	95	3.46	0.13	3.37	1.22	1.32	7.68	2.49	4.36	b
L+M+W	89	4.07	0.14	3.98	1.35	1.38	7.18	2.98	5.02	c

Table A4. Shapiro–Wilk Normality Test

Test	W Statistic	p–value	Interpretation
Shapiro–Wilk	0.966	< 0.001	Slight deviation (acceptable with large n)

Table A5. Levene's Test for Homogeneity of Variance

Test	F Statistic	df_1, df_2	p–value	Interpretation
Levene's Test	1.37	4, 442	0.243	Homogeneous variance

Table A6. ANOVA for CO_2 flux

Source	df	Sum of Squares	Mean Square	F–value	p–value
Treatment	4	87.39	21.847	14.1	< 0.001
Residuals	442	684.85	1.549	—	—
Total	446	772.24	—	—	—

Table A7. Tukey HSD pairwise comparisons

Comparison	Mean Diff.	95% CI Lower	95% CI Upper	Adj. p–value	Significant
L+M vs. Untreated	0.43	–0.09	0.95	0.160	No
L+M+B vs. Untreated	0.79	0.29	1.30	< 0.001	Yes
L+M+B+AMF vs. Untreated	0.73	0.23	1.24	< 0.001	Yes
L+M+W vs. Untreated	1.35	0.84	1.86	< 0.001	Yes
L+M+B vs. L+M	0.36	–0.16	0.88	0.318	No
L+M+B+AMF vs. L+M	0.30	–0.21	0.82	0.493	No
L+M+W vs. L+M	0.91	0.39	1.44	< 0.001	Yes
L+M+B+AMF vs. L+M+B	–0.06	–0.56	0.44	0.998	No
L+M+W vs. L+M+B	0.55	0.05	1.06	0.024	Yes
L+M+W vs. L+M+B+AMF	0.61	0.11	1.11	0.008	Yes

Table A8. Multiple regression coefficients

Predictor	Estimate	SE	t–value	p–value	Std. β	VIF
Intercept	–107.600	25.5300	–4.22	< 0.0001	—	—
T1 (Soil Temp, °C)	0.043	0.0061	7.10	< 0.0001	0.313	1.06
V4 (Moisture Voltage)	2.314	0.4020	5.76	< 0.0001	0.31	1.06
P (Pressure, kPa)	1.126	0.2660	4.23	< 0.0001	0.176	1.06

Table A9. Model summary statistics

Statistic	Value
Multiple R^2	0.187
Adjusted R^2	0.182
F–statistic	33.98
Degrees of freedom	3, 443
p–value	< 0.0001
RMSE	1.19 $\mu mol \cdot m^{-2} \cdot s^{-1}$

Table A10. Variance partitioning results

Component	Adj. R^2	% Explained	Unique %
Treatment Effects (ANOVA only)	0.105	10.5	7.8
Environmental Factors (Regression only)	0.182	18.2	15.5
Combined Model (Treatment + Environment)	0.289	28.9	—
Residual Variance	—	71.1	—
Total Variance	—	100.0	—